

## **Supporting Information**

### **Carrier Transport at the Metal-MoS<sub>2</sub> Interface**

Faisal Ahmed<sup>1,2</sup>, Min Sup Choi<sup>1,3</sup>, Xiaochi Liu<sup>1,3</sup> and Won Jong Yoo<sup>1,2,3,\*</sup>

<sup>1</sup>Samsung-SKKU Graphene Center (SSGC), SKKU Advanced Institute of Nano-Technology (SAINT),  
Sungkyunkwan University, 2066, Seobu-ro, Jangan-gu, Suwon, Gyeonggi-do, 440-746, Korea

<sup>2</sup>School of Mechanical Engineering, Sungkyunkwan University, 2066, Seobu-ro, Jangan-gu, Suwon,  
Gyeonggi-do, 440-746, Korea

<sup>3</sup>Department of Nano Science and Technology, SKKU Advanced Institute of Nano-Technology (SAINT),  
Sungkyunkwan University, 2066, Seobu-ro, Jangan-gu, Suwon, Gyeonggi-do, 440-746, Korea

\*Corresponding email: [yoowj@skku.edu](mailto:yoowj@skku.edu)

### S1 (R<sub>c</sub>-T Plot of Pd-MoS<sub>2</sub> contact)

Figure S1(a) is the OM image of the Pd/Au contacted device with 9nm thick MoS<sub>2</sub> flake as channel for carrier transport with lengths of 1, 1.5, 2, 2.5, 3 μm respectively. Figure S1(b) shows R<sub>c</sub>(T) of Pd-MoS<sub>2</sub> junction and a similar trend to that of Cr-MoS<sub>2</sub>, indicating thermionic emission dominant up to 215K followed by tunneling at low temperature.

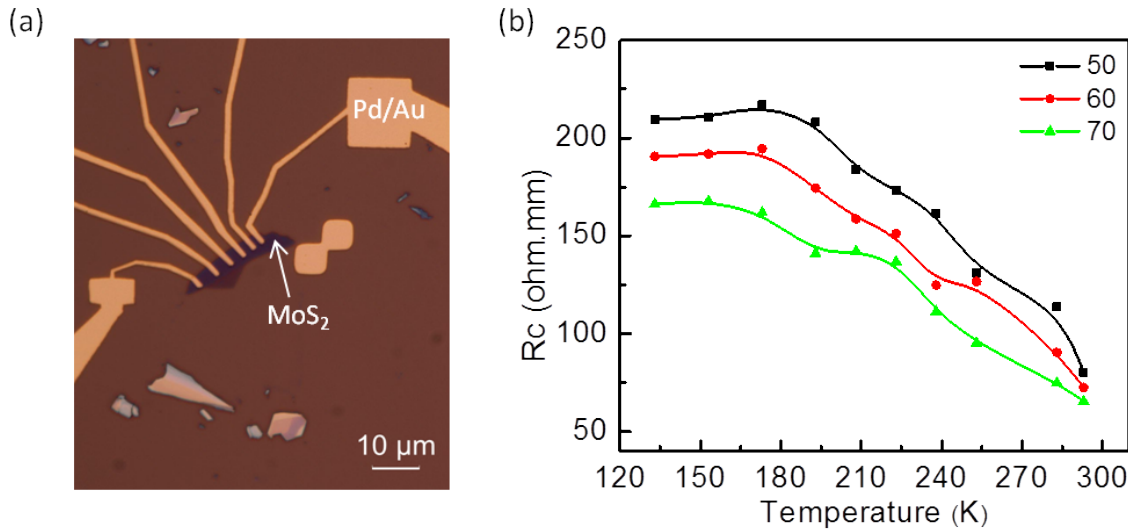


**Figure S1(a)** OM image of TLM patterned device with Pd/Au electrode and MoS<sub>2</sub> as channel. **(b)** the measured contact resistance of the device. Note that the drain bias is swept from -1 to 1 V during output curve measurement.

The higher value of R<sub>c</sub> in Fig. S1(b) can be attributed to the large barrier formed across the Pd-MoS<sub>2</sub> contact due to high work function of Pd (5.0eV) with respect to MoS<sub>2</sub>.

## S2 (Theoretical calculation of current across Cr-MoS<sub>2</sub> interface)

Das *et al* proposed the carrier transport model for holes conduction across metal-MoS<sub>2</sub> interface,<sup>1</sup> but here we implemented that model to the electron conduction at the interface.

The current along the barrier is extracted in three components, one thermionic emission ( $I_{TH}$ ) current and two of tunneling components ( $I_{TN-1}$  and  $I_{TN-2}$ ), as shown in Fig. 3(a) of the main manuscript and they are measured by the following equations.

$$I_{TH} = q \int_{\Phi_B}^{\chi} M(E + \Psi_{DRIVE} - \Phi_B) f(E) dE \quad (1)$$

$$M(E) = \frac{2}{h^2} \sqrt{2m^* E} \quad \text{and} \quad f(E) = \frac{1}{1 + \exp(\frac{E}{k_B T})}$$

$$I_{TN-1} = q \int_{\Phi_B - E_g}^{\Phi_B} M(E + \Psi_{DRIVE} - \Phi_B) T_1(E) f(E) dE \quad (2)$$

$$T_1(E) = \exp\left(-\frac{8\pi}{3h} \sqrt{2m^* (\Phi_B - E)^3} \times \frac{\lambda}{\Psi_{DRIVE}}\right)$$

$$I_{TN-2} = q \int_{\Phi_B - \Psi_{DRIVE}}^{\Phi_B - E_g} M(E + \Psi_{DRIVE} - \Phi_B) T_2(E) f(E) dE \quad (3)$$

$$T_2(E) = \exp\left(-\frac{8\pi}{3h} \sqrt{2m^* E_g^3} \times \frac{\lambda}{\Psi_{DRIVE}}\right)$$

$$\Psi_{DRIVE} = q \left[ V_D + |(V_G - V_{MIN} - V_{FB}) / \gamma| \right] \quad (4)$$

$$\lambda = \sqrt{t_{ox} t_{body} \times \frac{\epsilon_{body}}{\epsilon_{ox}}} \quad (5)$$

$$R_c = 1 / I \cdot q \quad (6)$$

Here,  $q$  is the charge of electron,  $\Phi_B$  denotes the Schottky barrier height for electrons,  $\chi$  is the electron affinity of MoS<sub>2</sub>,  $M(E)$  is the number of conduction modes in (eV.m.s)<sup>-1</sup>,  $f(E)$  is the Fermi-Dirac constant,  $m^*$  is the effective mass of electrons in MoS<sub>2</sub>,  $T_1(E)$  and  $T_2(E)$  are the tunneling efficiencies of carriers over their respective regions,  $\Psi_{DRIVE}$  denotes the amount of band bending by applied bias,  $\gamma$  is the band movement factor,  $V_{FB}$  is the flat band voltage and  $\lambda$  is the screening length extracted from equation (5). The parameter values used in our calculations are given in table S1. However,  $V_{MIN}$ ,  $V_{FB}$ ,  $\gamma$  and  $\Psi_{DRIVE}$  are calculated from transfer curve [Fig. S2 (a) and (b)]. The flat band voltage is approximately equal to the point at which the slope of  $\log(I_d)$  versus  $V_g - V_{MIN}$  deviates from linearity *i.e.* 2.9V in Fig. S2(b) and using the linear region slope that is equal to the  $60\gamma$  mV/decade,  $\gamma$  is extracted. For our device, it is around 23.8 and  $\Phi_B$  is extracted from thermionic emission theory [Fig. S2(c)].

**Table S1. Parameter values used in this work**

Gate oxide thickness ( $t_{ox}$ )	285 nm
Dielectric constant of SiO <sub>2</sub> ( $\epsilon_{ox}$ )	3.9
Body thickness ( $t_{body}$ )	14 nm
Dielectric constant of body ( $\epsilon_{body}$ ) <sup>1</sup>	7.0
Effective mass ( $m^*$ ) <sup>1</sup>	0.46m
Schottky barrier height ( $\Phi_B$ )	0.05 eV
Electron affinity ( $\chi$ )	4.0 eV
Band gap ( $E_g$ )	1.2 eV

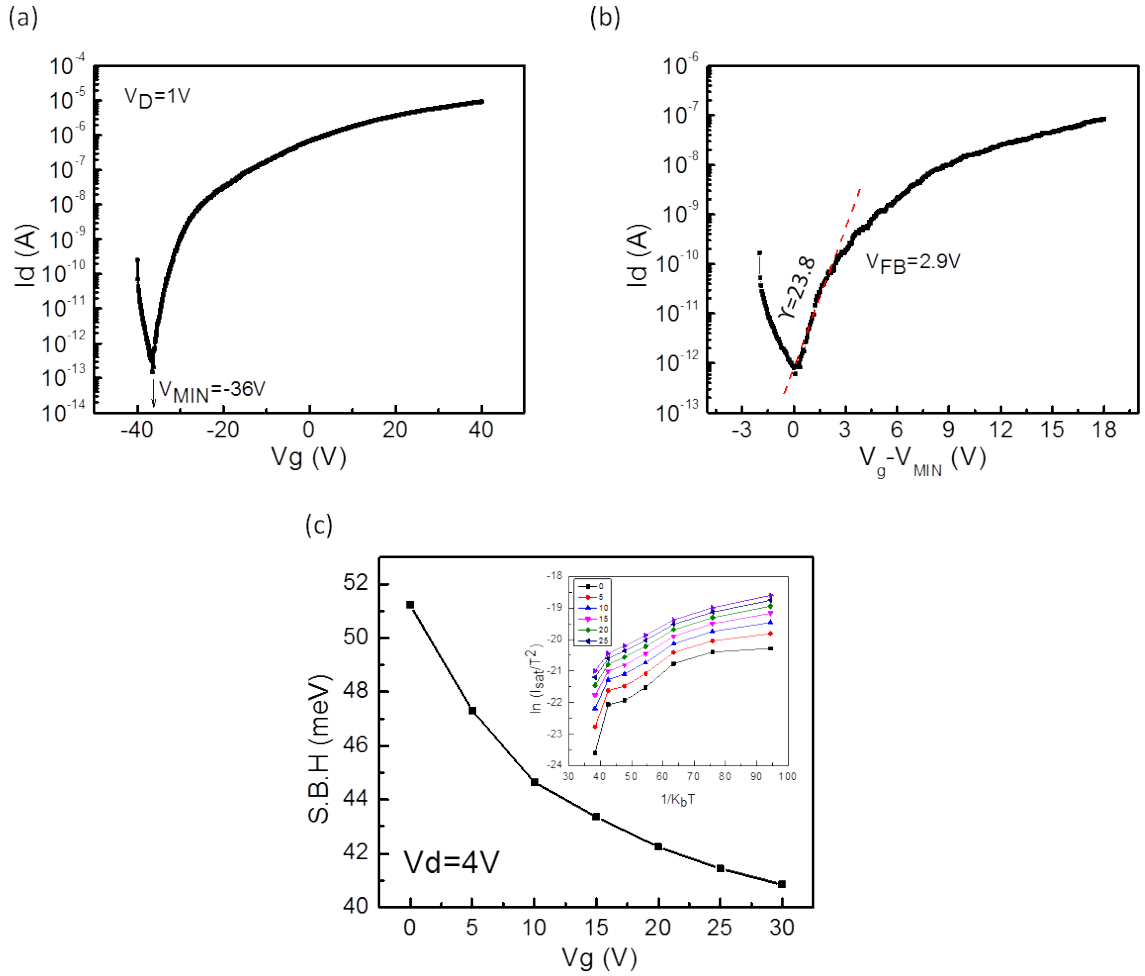


**Figure S2 (a)** The transfer curve of Cr-MoS<sub>2</sub> device on log scale showing typical n-type behavior.  $V_{\text{MIN}}$  is the gate bias at off-state of the device. **(b)** The calculation of flat band voltage ( $V_{\text{FB}}$ ) and band bending factor ( $\gamma$ ). **(c)** The calculated effective energy barrier variation against gate bias . Inset shows Arrhenius plot. Note that long channel ( $L_4$ ) is used for these measurements.

From detailed temperature measurement, Schottky barrier height is extracted using thermionic emission theory.<sup>2</sup> The extracted barrier height for electrons is about 50 meV at estimated flat band voltage as shown in Fig. S2 (c) . The small value of barrier height can be attributed to the Fermi level pinning effect, *i.e.* the Fermi level at the interface is pinned very near to the conduction band edge of MoS<sub>2</sub>.

The extracted values of all these parameters are used in equations from 1 to 5 to calculate all three current components as shown in the band diagram of Fig. 3(a) of the main manuscript, and their results are shown in Fig. 3(b) in units of A/m. Finally,  $R_c$  is extracted by applying the Landauer theory,<sup>3,4</sup> to the measured current components as shown in equation (6), and their results are shown in Fig. 3(c) in the units of ohm·mm except  $I_{TN-2}$ .

## References

1. S. Das, A. Parkash, R. Salazar and J. Appenzeller, *ACS Nano*, 2014, **8**, 1681–1689.
2. H.-M. Li, D.-Y. Lee, M. S. Choi, D. Qu, X. Liu, C.-Ho. Ra and W. J. Yoo, *Sci. Rep.*, 2014, **4**, 4041.
3. S. Datta, *Quantum transport: Atom to transistor*, Cambridge University press: New York, 2005.
4. M. Lundstrom, *Nanoscale transistors: device physics, modeling and simulation*, Springer: New York, 2006.